Partition instability in water-immersed granular systems

C. P. Clement, H. A. Pacheco-Martinez, Michael R. Swift, and P. J. King
School of Physics and Astronomy, University of Nottingham, Nottingham NG7 2RD, United Kingdom
(Received 30 April 2009; published 30 July 2009)

It is well known that a system of grains, vibrated vertically in a cell divided into linked columns, may spontaneously move into just one of the columns due to the inelastic nature of their collisions. Here we study the behavior of a water-immersed system of spherical barium titanate particles in a rectangular cell which is divided into two columns, linked by two connecting holes, one at the top and one at the bottom of the cell. Under vibration the grains spontaneously move into just one of the columns via a gradual transfer of grains through the connecting hole at the base of the cell. We have developed numerical simulations that are able to reproduce this behavior and provide detailed information on the instability mechanism. We use this knowledge to propose a simple analytical model for this fluid-driven partition instability based on two coupled granular beds vibrated within an incompressible fluid.

DOI: 10.1103/PhysRevE.80.011311 PACS number(s): 45.70.Mg, 47.55.Kf

I. INTRODUCTION

It is commonly observed that a system of grains under vertical vibration exhibits spatial instabilities [1]. In particular grains held in a space which is partitioned into segments linked by connecting holes may move into just one segment, the phenomenon of the "partition instability" [2–10]. There are a number of quite distinct physical mechanisms leading to this behavior.

The inelastic nature of granular materials has been shown to provide a mechanism for the partition instability [2]. Within a collection of kinetically active grains, dense regions will experience frequent dissipative collisions and the grains there will lose energy more rapidly than those in less dense regions. The system will spontaneously condense in the more dense regions which become even denser as they rapidly lose energy. This is the phenomenon of inelastic collapse [11,12]. Related behavior of this type is dramatically displayed by grains held in a vertically vibrated box which is divided by a vertical partition either of finite height or containing a small elevated hole [2–4]. If there are more grains on one side of the partition, then those grains will experience greater dissipation and be less kinetically active; they will bounce less high than those on the other side of the partition where there are fewer grains. This disparity in kinetic activity may cause a net flow of grains over the partition, or through the hole, from the minority side to the majority side. Under suitable conditions of vibration all of the grains may move to one side of the partition [2–4]. Similar behavior has also been observed within vibrated granular mixtures. Furthermore for particular vibratory conditions this instability may lead to periodic oscillatory motion of the grains from one side to the other [13–15].

In this paper we study a second mechanism which can give rise to a spatial instability, namely, the interaction between fine grains and a background fluid. This process may be illustrated using a fluid immersed granular bed within a vertically vibrating partitioned cell with two connecting holes, one at the top and one at the bottom of the cell. Under vibration the granular bed spontaneously moves into just one of the columns via a gradual transfer of grains through the connecting hole at the base of the cell.

Ohtsuki *et al.* [7] studied one such system consisting of fine grains in air vibrated within a partitioned container. They observed that the presence of air influences the height difference between the beds on either side of the container. Chen and Wei [8] suggested that this height difference may be due to the air-driven mechanism of Pak *et al.* [16], which was used to explain Faraday heaping [17]. Akiyama *et al.* [9] carried out a detailed study of the influence of air on the behavior of vertically vibrated grains in a symmetrically partitioned box. Unfortunately, the granular convection allowed by their wide box dimensions may well have contributed to the complex phenomena which they observed.

Here, we present an experimental and computational study of a water-immersed bed of barium titanate spheres vibrated within a partitioned cell in which the two identical columns are linked by two holes, one at the base and, importantly, a further hole in the partition, positioned well above the grains to allow fluid circulation. The two columns are of restricted horizontal dimensions to reduce the effects of tilting and of convection currents. Over a range of frequencies and amplitudes of vibration, we observe that the granular bed spontaneously moves into one of the columns so that few grains occupy the opposing column.

The use of a fluid such as water offers a number of advantages for investigating partition instabilities. First, water enables larger particles to be used, making the observation of the granular dynamics considerably simpler than for air. For nonturbulent fluid flow, the effects of fluid drag on the granular dynamics scale approximately as $\rho_g d^2/\eta$, where ρ_g is the density of the granular material, d is the grain diameter, and η is the dynamic viscosity of the surrounding fluid [18]. At 20 °C, water is about 50 times more viscous than air. This suggests that similar effects may be observed in water for particles ~7 times larger in diameter than for the equivalent behavior exhibited by fine particles in air.

The increased damping provided by a liquid such as water [19] reduces the granular temperature of a thrown bed maintaining the porosity, ϕ, closer to the value appropriate to a random packing of spheres. This makes comparison with the theory which we will develop later more straightforward than would be the case for a fluid such as air. Finally, the use of water eliminates the effects of static electricity which of-

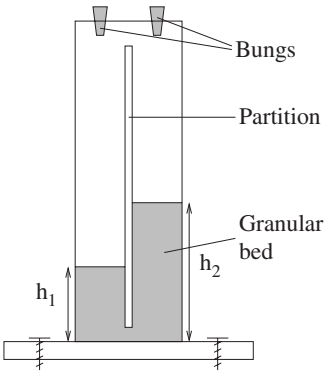

FIG. 1. Schematic representation of the experimental partitioned cell as described in the text.

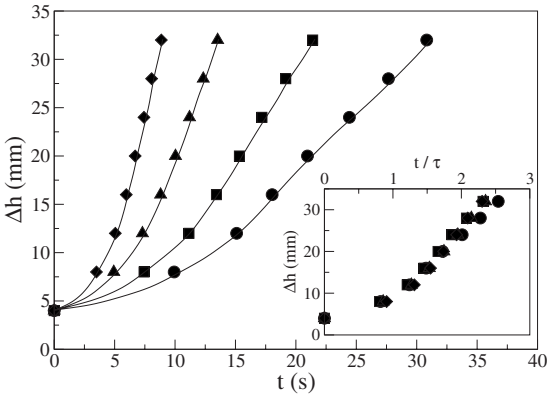

FIG. 2. The variation in height difference Δh as a function of time for a system of barium titanate grains fully immersed in water. The cell was vibrated at $f=15$ Hz and, from right to left, $\Gamma=2.25$ (circles), $\Gamma=2.50$ (squares), $\Gamma=3.00$ (triangles), and $\Gamma=3.50$ (diamonds). The size of the data points represent the errors in the measurements and the solid lines are a guide to the eyes. The inset shows that the data can be collapsed onto a single curve as described in the text.

ten slow and otherwise modify the dynamics of dry granular systems when they are shaken vigorously for long periods, particularly within an insulating box [18].

The rest of the paper is outlined as follows. In Sec. II we describe the experimental methods used to investigate the partition instability for which the results are presented in Sec. III. Section IV describes simulation techniques employed to model this system. Details of the validation of the simulation technique are given in Sec. V and the key results and findings are discussed in Sec. VI. Within Sec. VII we describe the mechanism for the instability. Section VIII introduces an semianalytical approach which can be used to model the instability. Finally a summary is given in Sec. IX.

II. EXPERIMENTAL METHODS

The experiments are conducted in a water-tight partitioned cell constructed from polymethyl methacrylate (PMMA), a cross section of which is shown schematically in Fig. 1. The cell is divided into two columns of identical dimensions by a central partition, each column being 90 mm high and 10 mm by 10 mm in horizontal cross section. The columns are linked by a gap at the bottom of the central partition, spanning the depth of the cell from front to back. The gap is 4 mm high and 10 mm in depth while the partition is 2 mm thick. A further substantial 7 mm gap spanning the depth of the cell at the top of the partition allows the free flow of fluid between the two columns in a region above the grains.

The experiments have been performed using spherical barium titanate grains of density 4500 kg m^{-3} and diameters spanning the range 600–850 μm to avoid gross crystallization effects. The grains are inserted into the cell through one of two upper holes. The cell is then filled with water of density 1000 kg m^{-3} and viscosity $\eta=8.91\times10^{-4}$ kg m^{-1} s^{-1}, which has been pumped prior to experiments to remove dissolved air. The cell is shaken to release any air bubbles trapped within the grains and then refilled and sealed with bungs so that no visible air bubbles are contained within its volume. The total amount of grains is such that $h_1+h_2=40$ mm, and they are distributed between the two columns so that the beds are given an initial height difference of $h_2-h_1=4$ mm. Here h_i is the height of the granular bed within column i, as shown in Fig. 1.

During experiments the cell is vibrated sinusoidally with frequency f in a direction aligned to within $\pm0.2°$ of vertical in a manner that ensures accurate one-dimensional motion [18]. The motion is monitored using cantilever capacitance accelerometers which display the dimensionless maximum acceleration $\Gamma=A\omega^2/g$. Here A is the amplitude of vertical vibration, $\omega=2\pi f$ is the angular frequency, and g is the gravitational acceleration.

Vibration is applied and the height of the granular beds in the left and right columns are studied as a function of the total time of vibration, the heights being measured through the use of a high-speed camera. This camera, usually operated at 1000 frames per second, also allows the study of granular motion within each cycle.

III. EXPERIMENTAL RESULTS

As we vibrate the system we find that over time the particles migrate through the lower hole from the shallower bed into the taller bed. Eventually almost all the grains occupy just one of the columns, with only a small percentage of grains inhabiting the gap and the base of the opposite column. By analyzing footage from the high-speed camera we have observed in detail the motion of grains between columns within each cycle. In the first part of the cycle the grains are thrown and particles are drawn from the shallower to the deeper bed while both beds are in flight. In the second part of the cycle as the two beds land a smaller number of particles are forced back toward the shallower bed. On average we find that the motion of grains is greater during flight than on landing, thus the particles gradually migrate from the shallower to the deeper granular bed.

We define $\Delta h=|h_1-h_2|$ as the magnitude of the difference in height between the two granular columns. Figure 2 plots Δh against time, t, for barium titanate in water vibrated at $f=15$ Hz with accelerations in the range $\Gamma=2.25-3.5$. The

plot shows that the transfer of grains into the deeper bed initially accelerates as Δh increases and then continues at an almost constant rate until almost all the grains are in the deeper bed. Subsequently the net transfer of grains decelerates until a steady state is reached in which a small number of grains move backward and forward between the two columns. The last experimental points we plot are at $\Delta h = 32$ mm as beyond this point the results become erratic and difficult to measure.

Unsurprisingly we find that as Γ is increased the total time taken for the grains to migrate into one column reduces due to the increased amount of mechanical energy within the beds driving the grain transfer process. The inset to Fig. 2 shows that the data for different values of Γ can be collapsed onto a single curve when plotted against a rescaled time t/τ, where $\tau = 100\Gamma^{-2.6}$ s. This strong dependence on Γ results from the nonlinear flight dynamics of the bed within the fluid and the variation in bed porosity with vibratory conditions.

We note that, when experiments are performed with the gap through the partition at the top of the cell sealed, there is no transfer of grains from the shallower to the deeper granular bed. In fact if vibrated for a long period of time the granular beds then end up of equal height.

IV. SIMULATION TECHNIQUES

To gain insight into the physical mechanisms which lead to the instability formation, and in order to be able to study features not readily accessible from experiment, we have also carried out numerical simulations. Initially we tried to simulate the partition instability using a particle fluid model in which the fluid is described by the Navier-Stokes equations and the fluid particle coupling is introduced through the use of an empirical bed equation [20]. Models of this type have been used effectively to simulate Faraday piling and the separation of a binary mixture [21,22]. Using these models we were able to simulate the partition instability. However, we were unable to obtain even qualitative agreement with our experiments. This is because models based on a bed equation are unable to accurately describe the fluid and grain motion through the gap. The bed equations are empirical fits to macroscopic properties of fluid flow through porous media and are not applicable at the small scales needed to model flow through complex geometries as in the partition system. We have therefore employed an alternative simulation approach.

Here we describe a technique in which the fluid motion is resolved on a scale small compared to the particles and no macroscopic bed equation is required. This allows for greater accuracy in modeling particle-fluid flow in complex geometries. The method was first employed by Glowinski *et al.* [23–25] and further developed by Hofler and Schwarzer [26]. In this approach the fluid particle coupling is achieved by introducing a body forcing term into the Navier-Stokes equations rather than through providing a boundary condition for the fluid flow. This method has been used successfully in a range of contexts including sedimentation and filtration [25]. However, to our knowledge this method has so far not been used to simulate fully immersed vibrated granular beds. We will briefly outline the method that we have used before applying it to vibrated granular systems.

The fluid, with flow velocity $\mathbf{v}$, is assumed to be incompressible, $\boldsymbol{\nabla}\cdot\mathbf{v}=0$, and described by the 3D Navier-Stokes equation

$$\frac{\partial \mathbf{v}}{\partial t} + (\mathbf{v}\cdot\boldsymbol{\nabla})\mathbf{v} = -\frac{1}{\rho}\boldsymbol{\nabla} P + \nu\nabla^2\mathbf{v} - \frac{1}{\rho}\mathbf{f}. \tag{1}$$

Here ρ, ν, and P are the fluid density, kinematic viscosity, and pressure, respectively, and $\mathbf{f}$ is the volume force used to implement particle fluid coupling. These equations are spatially discretized on a staggered marker and cell (MAC) mesh [27] and solved using the projection method [26].

The basic idea of this model is to allow the fluid to exist both inside and outside the particles. The particles are therefore treated not as boundary conditions to the flow but by a volume forcing term, $\mathbf{f}$, in the Navier-Stokes Eq. (1). Note that the fluid is resolved on a scale much smaller than the particles, unlike the bed equation models discussed above.

The first step in coupling the fluid and particle motion is to represent each particle by a set of points that moves with the particle. We use n reference points distributed over the volume of each particle. For particle i the spatial coordinates of these points are $\mathbf{x}_{ij}$, $j=1,\ldots,n$. In our implementation we ignore particle rotation such that the $\mathbf{x}_{ij}$ only change due to the translational motion of the particle.

The fluid particle coupling is introduced by forcing the fluid within each particle to move as closely with the particle as possible. At each point $\mathbf{x}_{ij}$ the particle has a velocity $\mathbf{u}_{ij}$ and the fluid has a velocity $\mathbf{v}_{ij}=\mathbf{v}(\mathbf{x}_{ij})$. In order to determine $\mathbf{v}_{ij}$ at an arbitrary point in space a linear interpolation from the staggered fluid grid has been used. If there were no fluid-particle coupling the particle and fluid would follow different paths and, after a time Δt, would be separated by a displacement $\boldsymbol{\epsilon}_{ij}=(\mathbf{v}_{ij}-\mathbf{u}_{ij})\Delta t$. To limit the separation we introduce a body force term on the fluid given by

$$\mathbf{f}_{ij}(\mathbf{x}_{ij}) = -k\boldsymbol{\epsilon}_{ij} - 2\gamma\dot{\boldsymbol{\epsilon}}_{ij}. \tag{2}$$

Here k is a spring constant and γ is a damping constant. This form of interaction effectively introduces a damped "spring" between the reference point on the particle, $\mathbf{x}_{ij}$, and the corresponding point within the fluid.

To conserve momentum we see that an equal and opposite force must be applied to the particle at each reference point. Thus a force

$$\mathbf{F}_{ij} = k\boldsymbol{\epsilon}_{ij} + 2\gamma\dot{\boldsymbol{\epsilon}}_{ij} \tag{3}$$

acts upon the particle i at the location of reference point j. For a particle of volume V_i, we must also add a force to explicitly account for gravity and buoyancy

$$\mathbf{F}_i^S = (\rho - \rho_g)V_i\mathbf{g}, \tag{4}$$

where $\mathbf{g}$ is the acceleration due to gravity.

The total force $\mathbf{F}_i$ on particle i is given by $\mathbf{F}_i=\mathbf{F}_i^S+\mathbf{F}_i^C+\Sigma_{j=1}^n\mathbf{F}_{ij}$, where $\mathbf{F}_i^C$ is the force contributions from collisions with other particles and the cell walls. The interparticle collisions are modeled using a Hertzian elastic repulsive force and damped using a viscoelastic force as detailed by Ku-

wawbara and Kono [28]. The spring constant we use is evaluated using measurable particle properties; the Young's modulus and the Poisson ratio. The damping parameter was chosen so that the coefficient of restitution is 0.2 for a relative impact velocity of 0.25 m s^{-1}. Coulomb friction between particles is also included. Here the coefficient of friction μ was chosen to be 0.52 which was determined experimentally from angle of repose measurements.

To integrate the equations of motion for the translation of each particle we use Verlet's method. To improve numerical efficiency, we use a time step of $\Delta t=5.0\times10^{-7}$ s to resolve the particle motion while using $\Delta t=1.0\times10^{-4}$ s for the fluid motion. The fluid lattice spacing Δ we use is 1.166×10^{-4} m, implying that there are approximately $n=115$ reference points contained in the volume of each particle. The values of the spring constant and damping parameter between the fluid and particle are $k=0.165$ kg s^{-2} and $\gamma=2.99\times10^{-7}$ kg s^{-1}. The code was developed in house and a typical simulation takes two to three weeks to run on a high-end PC.

V. VALIDATION OF THE MODEL

As a validation of the fluid spring (FS) model we simulate a thrown bed within a single column and compare the results with both experimental data and those obtained with the theoretical Kroll model [29]. Kroll developed an analytic description for the dynamics of a fluid-immersed thrown granular bed. Here we briefly outline this model.

A. Kroll model

Kroll considered a granular bed being thrown vertically from a platform undergoing sinusoidal motion, the bed moving purely in the vertical direction within a massless incompressible fluid. He supposed that the bed could be considered as a rigid porous plug which was thrown, landed, and settled within each cycle of vibration. Friction between the bed and the sidewalls of the container is ignored. We consider a bed of depth h and uniform porosity ϕ being thrown from a platform moving as $z_c=A\sin(\omega t)$. During flight the bottom of the bed is at $z(t)$. In response to the motion of the bed, fluid is drawn through it producing a pressure difference ΔP across the bed. The pressure difference ΔP may be related to the superficial fluid velocity v through the use of a bed equation,

$$\Delta P = K(v)hv. \tag{5}$$

Here the permeability $K(v)$ is a function of $|v|$, ϕ, the particle size, and the fluid viscosity. The application of Newton's laws to the motion of the bed gives

$$\rho_g(1-\phi)h\ddot{z} = -\rho_g(1-\phi)hg + \Delta P. \tag{6}$$

Here ρ_g is the density of the granular material, the first term on the right-hand side is the force on the bed due to gravity and the second term is the pressure force. Further, conservation of fluid volume yields the equation

$$\dot{z} - \dot{z}_c + v = 0. \tag{7}$$

Equations (5)–(7) are combined to give an equation for the motion of the bed,

$$\dot{u} + K'(u)u + g = -\ddot{z}_c, \tag{8}$$

where $u=\dot{z}-\dot{z}_c$ is the rate of change in the gap between bed and platform with respect to time. If required u may readily be integrated to yield the gap itself. In Eq. (8) $K'(u)=K(u)/[\rho_g(1-\phi)]$.

The treatment of Kroll assumes that the fluid is massless. Inclusion of a nonzero fluid density modifies a number of the terms in Eq. (8) by numerical factors [30], giving

$$\beta\dot{u} + K'(u) + \alpha g = -\alpha\ddot{z}_c. \tag{9}$$

The factor $\beta=1+\frac{\rho_f}{\rho_g}\frac{1-\phi}{\phi}$ is an effective mass correction, while $\alpha=\frac{(\rho_g-\rho_f)}{\rho_g}$ is a correction due to buoyancy. This expression does not contain h as, in this model, beds of different heights follow the same flight trajectory. We note that for a dense bed of water-immersed barium titanate grains for which $\phi\approx0.42$, the parameters α and β are about 0.78 and 1.31, respectively. Equation (9) can be solved numerically to determine the trajectory of the bed and the pressure variation throughout the cycle can be obtained from Eq. (5).

B. Dynamics of a single-vibrated column

In order to validate the FS model we consider a single column containing a granular bed vibrated at $f=15$ Hz and $\Gamma=2.5$. The bed consists of spherical barium titanate particles with diameters in the range 600–850 μm and density $\rho_g=4500$ kg m^{-3}. To obtain experimental results the granular beds are vibrated within a cylindrical cell of internal diameter of 10 mm. The cell has pressure sensors at the bottom and top to enable the pressure drop across the bed to be determined during flight. The depth of the granular column at rest is 20 mm. In our simulations we use a cell with square cross section of dimensions 4 mm$\times$4 mm which allows us to simulate a bed having the same depth as in experiment. Frictional effects with the side walls are omitted. For comparison the same parameters as used in simulation and experiment are used in the buoyancy corrected Kroll model. We use Ergun's bed equation [31] to determine $K'(u)$ so that

$$K'(u) = \frac{180(1-\phi)\eta}{\phi^3\rho_g d^2} + \frac{1.75\rho}{\phi^3\rho_g d}|u|. \tag{10}$$

We then calculate the bed flight from Eq. (8) and ΔP from Eq. (5).

Figure 3 plots ΔP across the granular bed against the phase angle of vibration θ over the course of one cycle. We define the beginning of the cycle $\theta=0°$ as the point when the base is moving upwards at maximum velocity; at this time the bed sits on the cell base. The different curves correspond to the analytical Kroll model, the FS model simulation, and experimental results obtained with the cylindrical cell. The results obtained with the FS model were averaged over 40 cycles, while the experimental data were averaged over 128. There is good agreement between the simulated curve and the Kroll model which shows that even though the FS model does not include an empirical bed equation it is still able to predict the bed motion in an accelerated system. Simulations of this type could therefore be used to study flow through

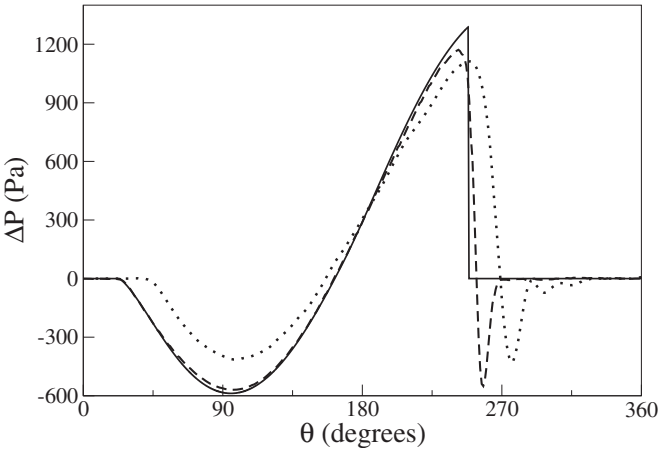

FIG. 3. The under pressure ΔP against the phase angle θ throughout a cycle for vibration parameters $f=15$ Hz and $\Gamma=2.5$. The different curves correspond to experimental data within a narrow box (dotted line), simulation results from the FS model (dashed line) and the buoyancy corrected Kroll model (solid line).

porous media under a wide range of conditions. The slight difference between the experimental curve and the Kroll model is due to wall friction effects in the narrow box. Note, however, that if a wider box is used the surface develops a Faraday tilt and a direct comparison with the Kroll model is no longer possible.

VI. TWO-COLUMN SIMULATION

We now describe simulations of a two column system similar to that used in the experiments described above. Each column has the same width and height as in experiment, 10 and 90 mm, respectively, while the depth of the cell from front to back is reduced to 2.5 mm to aid computational speed. The connecting gaps between the two columns at the base and top of the container both have a width of 2 mm and respective heights of 4 and 7 mm. We use 2700 barium titanate particles with diameters spanning the range 600–850 μm to prevent crystallization. At rest the total height of both columns is 40 mm. The container is vibrated sinusoidally at $f=15$ Hz for several values of Γ.

Figure 4 shows the evolution of the partition instability for $\Gamma=2.5$ at times of $t=0$, 10, and 25 s. The columns are given an initial height difference of $\Delta h=4$ mm as in experiments. At $t=10$ s the grains have appreciably transferred into the right-hand column and by $t=25$ s almost all of the grains in the left-hand column have moved through the gap in the base into the right-hand column. At this point the columns are in dynamic equilibrium.

Figure 5 plots Δh against time for vibration parameters $f=15$ Hz and $\Gamma=2.25, 2.50, 3.00, 3.50$ for the FS model simulations. We have also included the results from experiments within the figure. Here we see that the agreement between simulation and the experimental results is very good, except at the lowest value of Γ used, 2.25. For this value of Γ the agreement is not as good, which we believe is due to the fact that in the experiments the barium titanate grains are slightly non-spherical and tend to jam within the gap. At low

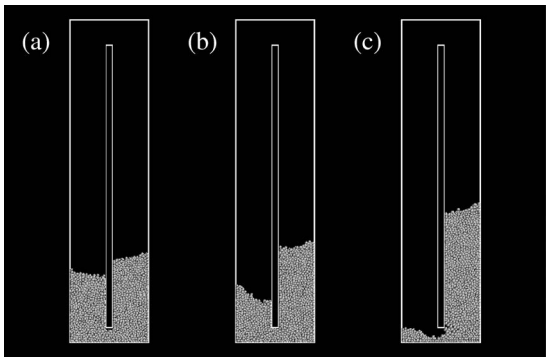

FIG. 4. Snapshots from simulation showing the time evolution of 2700 water-immersed barium titanate particles of diameter 600–850 μm vertically vibrated within the partitioned cell at $f=15$ Hz and $\Gamma=2.5$. The timings are (a) $t=0$ s, (b) $t=10$ s, and (c) $t=25$ s.

Γ there is not enough agitation to maintain the smooth flow of grains found at higher Γ. Given the good agreement between simulations and experiments we will now use simulations alone to investigate in detail the instability mechanism.

VII. INSTABILITY MECHANISM

We now consider the possible mechanism for the partition instability. Two limiting cases can readily be described. In the first, the resistance to fluid flow through the bottom gap far exceeds that through either bed. Under vibration each granular column is thrown independently and will develop an under pressure proportional to its height. The pressure drop under the deeper bed early in flight will be greater than beneath the shallower bed, as follows from Eq. (5), causing grains to move in the direction of the deeper bed. Later in flight the changing pressure reduces the particles' velocities but is not sufficient to reverse the direction of grain motion. A second possibility is that the coupling between the two columns is such that the resistance to fluid flow through the lower hole is far less than that through either bed. Both columns experience a common under pressure which can only

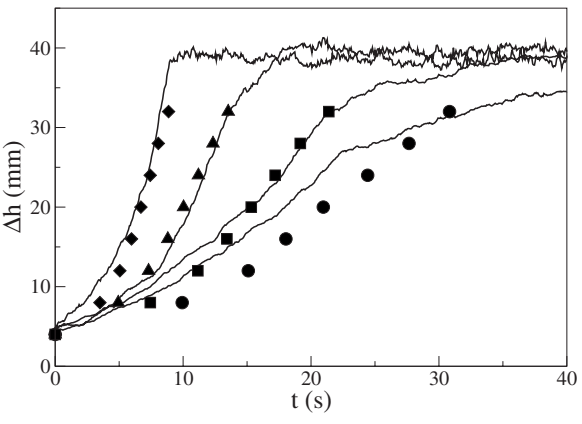

FIG. 5. Variation in Δh with time, t at $f=15$ Hz. Solid curves from right to left are for $\Gamma=2.25$, 2.50, 3.00, and 3.50. The experimental data has also been plotted for comparison.

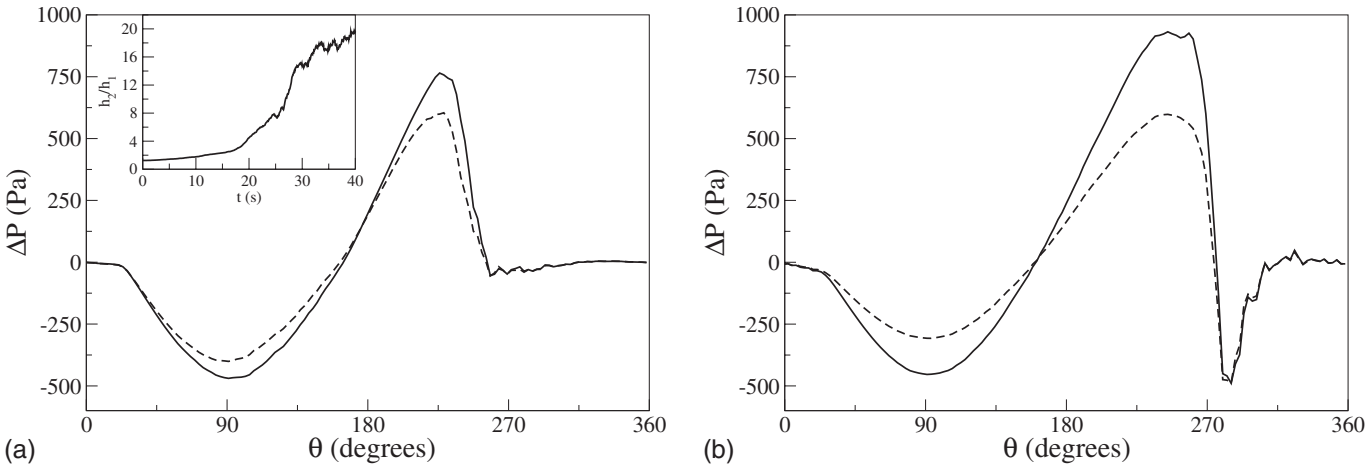

FIG. 6. Under pressure drop across the bed on each side of the partition plotted against the phase angle θ for the deep column (solid line) and the shallow column (dashed line). The vibration parameters are $f=15$ Hz and $\Gamma=2.5$ and the figures show data at times (a) $t=10$ s and (b) $t=30$ s. The data was averaged over 5 cycles. The insert in (a) shows the height ratio h_2/h_1 against time, t.

be achieved if more fluid flows through the shallower bed rather than through the deeper bed. This fluid flow also transports grains toward the deeper granular column.

In order to test which, if either, mechanism is dominant we determine from simulation the pressure beneath each column for vibrational parameters $f=15$ Hz and $\Gamma=2.5$. Figures 6(a) and 6(b) show the pressure drop across the bed on each side of the partition at times $t=10$ s and $t=30$ s. The inset in Fig. 6(a) shows the variation in h_2/h_1 with time t. The variation in pressure throughout a cycle shows that ΔP is approximately the same on both sides of the partition. For example, by $t=30$ s the height ratio is $h_2/h_1 \approx 15$, while the ratio of pressures on the two sides $\Delta P_2/\Delta P_1$ is only 1.5. Furthermore, the pressure curves throughout a cycle on either side of the partition can be scaled onto each other. Figure 7 plots the ratio of pressure drops, $\Delta P_2/\Delta P_1$, across each bed against the ratio of the heights of the two bed depths, h_2/h_1, as grains move from one column to the other. The figure shows that as h_2/h_1 increases $\Delta P_2/\Delta P_1$ only increases slowly and eventually levels at approximately 1.55 as h_2/h_1 reaches 21. These results show that, for our experimental geometry, the resistance to fluid flow through the bottom gap is low, the second scenario described above. In the next section we propose an analytical model based on the Kroll model which captures this mechanism.

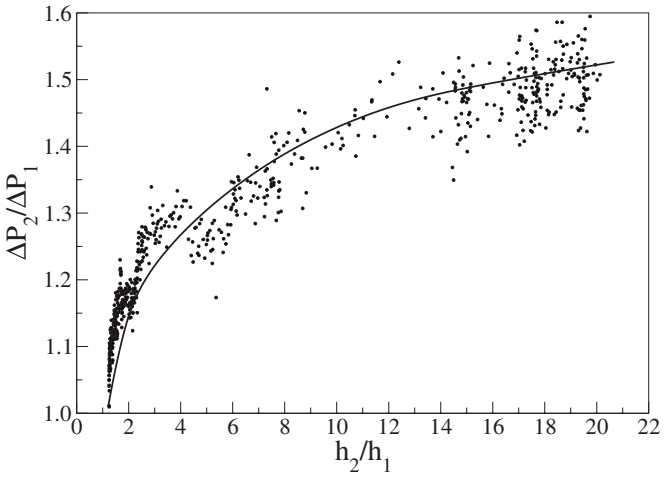

FIG. 7. Ratio of pressure drops, $\Delta P_2/\Delta P_1$, as a function of the height ratios h_2/h_1. The solid line is a guide to the eyes.

VIII. COUPLED COLUMN KROLL MODEL

In this section we propose a semi-analytical approach to model the transfer of grains between two coupled columns, namely, the coupled column Kroll model. The approach we use is based on the numerical Kroll model described in Sec. V. We extend these ideas to the present experimental situation that of two coupled columns, an arrangement shown schematically in Fig. 8 where the variables and parameters of the two columns are labeled as 1 and 2.

We suppose that the two beds experience under pressures ΔP_1 and ΔP_2 when in flight which may be related to the fluid flow through each bed such that we have $\Delta P_1 = h_1 K_1 v_1$ and

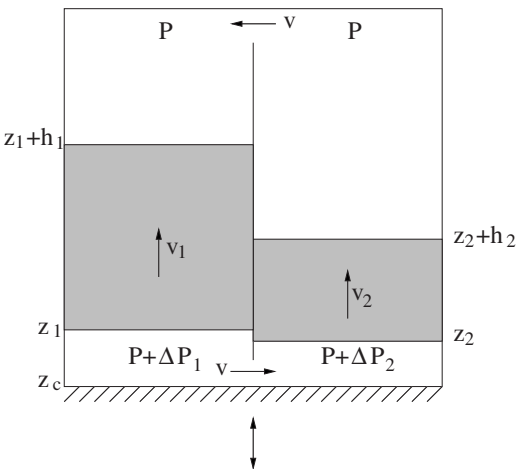

FIG. 8. Schematic diagram used to define the pressure, the positions of the beds and the fluid velocities within a two column system.

$\Delta P_2 = h_2 K_2 v_2$. Here v_i is the fluid flow through column i and K_i is the permeability of bed i. The pressure ratio consequently satisfies

$$\frac{\Delta P_2}{\Delta P_1} = \frac{h_2 K_2 v_2}{h_1 K_1 v_1}. \tag{11}$$

As noted above this pressure ratio is approximately constant throughout the transfer process. For simplicity we fix $\Delta P_2 / \Delta P_1 = 1.0$ [32].

Note that were the two columns to be connected by a long tube, the first case discussed above, this condition would be replaced by $\Delta P_2 / \Delta P_1 = h_2 / h_1$. In this limit the resistance to flow through the gap is high and the two beds are assumed to be thrown independently. Consequently the pressure drop across each bed is proportional to its depth.

During bed flight there will be a movement of fluid, at velocity v, through the lower coupling hole. For this to occur there must be a corresponding flow through the upper hole, high in the partition. Using variables $u_1 = \dot{z}_1 - \dot{z}_c$ and $u_2 = \dot{z}_2 - \dot{z}_c$, conservation of fluid volume requires that

$$u_1 + v_1 = -A_r v = -u_2 - v_2, \tag{12}$$

where A_r is the ratio of the cross-sectional areas of the channels to the lower coupling hole. Applying Newton's laws to the two beds as before we obtain

$$\dot{u}_1 + g = K_1' v_1 - \ddot{z}_c \tag{13}$$

and

$$\dot{u}_2 + g = K_2' v_2 - \ddot{z}_c. \tag{14}$$

While both beds are in flight Eqs. (11)–(14) may be solved to find u_1, u_2, v_1, and v_2. Using these values, v may be obtained from Eq. (12). To solve these equations K_i' was obtained using Eq. (10). It is found that the two strongly coupled beds do not follow the same flight path and that one lands before the other. We suppose that grains only move through the lower channel from one column to the other while both beds are in flight. An empirical fit to the data can be obtained if the rate of movement of grains from one column to the other is $cv\Gamma$, where c is a constant fitting parameter. The net transfer of grains during a cycle is assumed to be proportional to the volume flow of fluid through the hole and how strongly the bed is fluidized by the vibration. This model has been implemented numerically.

Figure 9 shows a comparison between the experimental data and the coupled column Kroll model. Here the single fitting parameter c has been chosen to be 0.0115. The analytical model provides a good fit to the experimental data. However, it is unable to accurately capture the final stage of the grain transfer when the rate begins to slow. As in experiment, the coupled column Kroll model data can be collapsed onto a single curve by rescaling time by $\tau = 100\Gamma^{-2.6}$ s.

The simulation results and analytical model enables us to better understand the mechanism which drives the grain transfer. When the beds are thrown, an under pressure develops across the base of the container and thus fluid flows downwards through the beds to fill the space left beneath. The shallower bed provides less resistance to the downward flowing fluid and thus fluid is drawn from the shallower side through the hole to the deeper side. The fluid accelerates grains in the direction of the flow, from the shallower to the deeper bed. As the beds begin to fall in the second half of the cycle an over pressure develops beneath the beds and the fluid flow is reversed. Fluid is forced upwards through the beds to fill the void above. Again the shallower bed provides less resistance to the upward moving fluid so fluid now flows through the channel from the deeper bed to the shallower bed. However, the shallower bed lands first, thus reducing the transfer of grains back from the deeper bed. Over a cycle there is a net transfer of grains from the shallower to the deeper bed, hence the instability. The process is repeated and accelerates as the increasing Δh leads to less resistance to fluid flow through the shallower bed and greater resistance through the deeper bed. Eventually an equilibrium is established when as many grains move into the deeper bed in the early part of the cycle as move back into the shallower bed when the grains land. At this stage the system is in dynamic equilibrium which usually occurs when the vast majority of grains reside in one column only.

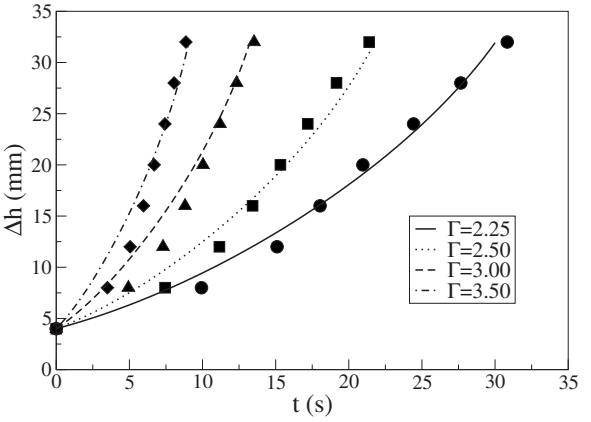

FIG. 9. Variation in Δh with time t obtained with the coupled column Kroll model. The cell was vibrated at $f = 15$ Hz and amplitudes in the range $\Gamma = 2.25 - 3.50$. The points show the corresponding experimental data.

IX. SUMMARY

We have investigated the water-driven partition instability, in which grains transfer from one side of a partitioned cell to the other through a lower connecting hole. We have developed simulations which are able to accurately model this process and provide insight into the instability mechanism. The transfer of grains results from the greater flow of fluid through the shallower bed of grains as the beds are thrown by the vibration. The behavior can be captured by a coupled column Kroll model.

[1] For a review, see K. van der Weele, Contemp. Phys. **49**, 157 (2008).
[2] J. Eggers, Phys. Rev. Lett. **83**, 5322 (1999).
[3] K. van der Weele, D. van der Meer, M. Versluis, and D. Lohse, Europhys. Lett. **53**, 328 (2001).
[4] D. van der Meer, K. van der Weele, and D. Lohse, Phys. Rev. Lett. **88**, 174302 (2002).
[5] T. Akiyama and T. Shimomura, Adv. Powder Technol. **4**, 129 (1993).
[6] Y. Maeno, Physica A **232**, 27 (1996).
[7] T. Ohtsuki, D. Kinoshita, Y. Nakada, and A. Hayashi, Phys. Rev. E **58**, 7650 (1998).
[8] W. Chen and R. Wei, Phys. Lett. A **244**, 389 (1998).
[9] T. Akiyama and T. Shimomura, Powder Technol. **66**, 243 (1991).
[10] T. Akiyama, K. Shinmura, S. Murakawa, and K. M. Aoki, Granular Matter **3**, 177 (2001).
[11] S. McNamara and W. R. Young, Phys. Rev. E **50**, R28 (1994).
[12] I. Goldhirsch and G. Zanetti, Phys. Rev. Lett. **70**, 1619 (1993).
[13] R. Lambiotte, J. M. Salazar, and L. Brenig, Phys. Lett. A **343**, 224 (2005).
[14] S. Viridi, M. Schmick, and M. Markus, Phys. Rev. E **74**, 041301 (2006).
[15] M. Hou, H. Tu, R. Liu, Y. Li, K. Lu, P. Y. Lai, and C. K. Chan, Phys. Rev. Lett. **100**, 068001 (2008).
[16] H. K. Pak, E. Van Doorn, and R. P. Behringer, Phys. Rev. Lett. **74**, 4643 (1995).
[17] M. Faraday, Philos. Trans. R. Soc. London **121**, 299 (1831).
[18] M. C. Leaper *et al.*, Granular Matter **7**, 57 (2005).
[19] P. Gondret, M. Lance, and L. Petit, Phys. Fluids **14**, 643 (2002).
[20] J. A. N. Kuipers, K. van Duin, F. van Beckum, and W. van Swaaij, Comput. Chem. Eng. **17**, 839 (1993).
[21] R. J. Milburn, M. A. Naylor, A. J. Smith, M. C. Leaper, K. Good, M. R. Swift, and P. J. King, Phys. Rev. E **71**, 011308 (2005).
[22] H. J. van Gerner, M. A. van der Hoef, D. van der Meer, and K. van der Weele, Phys. Rev. E **76**, 051305 (2007).
[23] R. Glowinski, T. W. Pan, and J. Periaux, Comput. Methods Appl. Mech. Eng. **112**, 133 (1994).
[24] R. Glowinski, T. W. Pan, T. I. Hesla, and D. D. Joseph, Int. J. Multiphase Flow **25**, 755 (1999).
[25] R. Glowinski *et al.*, Int. J. Numer. Methods Fluids **30**, 1043 (1999).
[26] K. Hofler and S. Schwarzer, Phys. Rev. E **61**, 7146 (2000).
[27] F. H. Harlow and J. E. Welch, Phys. Fluids **8**, 2182 (1965).
[28] G. Kuwabara and K. Kono, Jpn. J. Appl. Phys., Part 1 **26**, 1230 (1987).
[29] W. Kroll, Forsch. Geb. Ingeneiurwes. **20**, 2 (1954).
[30] A. J. Smith, M. C. Leaper, M. R. Swift, and P. J. King, Phys. Rev. E **71**, 031303 (2005).
[31] S. Ergun, Chem. Eng. Prog. **48**, 89 (1952).
[32] The small variation in the pressure ratio with height, shown in Fig. 7, can be included in the analytical model by using a best fit to the simulated data. However, such variation does not significantly change the predicted dependence of Δh on t.